ISSN 8755-6839

SCIENCE OF **TSUNAMI HAZARDS**

Journal of Tsunami Society International

Volume 31 **Number 2** **2012**

GEODYNAMICS OF NAZCA RIDGE'S OBLIQUE SUBDUCTION AND MIGRATION - IMPLICATIONS FOR TSUNAMI GENERATION ALONG CENTRAL AND SOUTHERN PERU: Earthquake and Tsunami of 23 June 2001

George Pararas-Carayannis
Tsunami Society International, Honolulu, Hawaii, USA

ABSTRACT

Peru is in a region of considerable geologic and seismic complexity. Thrust faulting along the boundary where the Nazca plate subducts beneath the South American continent has created three distinct seismic zones. The angle of subduction of the Nazca oceanic plate beneath the South American plate is not uniform along the entire segment of the Peru-Chile Trench. Furthermore, subduction is affected by buoyancy forces of the bounding oceanic ridges and fractures - such as the Mendana Fracture Zone (MFZ) to the North and the Nazca Ridge to the South. This narrow zone is characterized by shallow earthquakes that can generate destructive tsunamis of varied intensities. The present study examines the significance of Nazca Ridge's oblique subduction and migration to the seismicity of Central/Southern Peru and to tsunami generation. The large tsunamigenic earthquake of 23 June 2001 is presented as a case study. This event generated a destructive, local tsunami that struck Peru's southern coasts with waves ranging from 3 to 4.6 meters (10-15 feet) and inland inundation that ranged from 1 to 3 km. In order to understand the near and far-field tsunamigenic efficiency of events along Central/Southern Peru and the significance of Nazca Ridge's oblique subduction, the present study examines further the geologic structure of the region and this quake's moment tensor analysis, energy release, fault rupture and the spatial distribution of aftershocks. Tsunami source mechanism characteristics for this event are presented, as inferred from seismic intensities, energy releases, fault plane solutions and the use of empirical relationships. The study concludes that the segment of subduction and faulting paralleling the Peru-Chile Trench from about 15^0 to 18^0 South, as well as the obliquity of convergent tectonic plate collision in this region, may be the reason for shorter rupture lengths of major earthquakes and the generation of only local destructive tsunamis.

Keywords: *Peru earthquake, tsunami, Peru-Chile Trench, seismotectonics, Nazca Ridge*

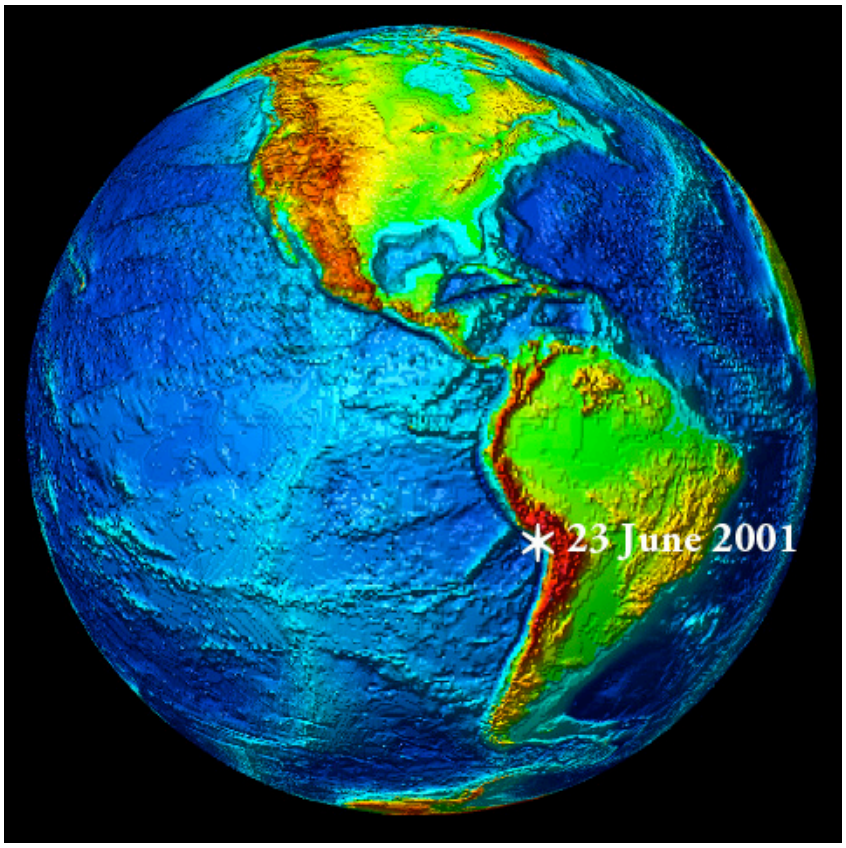

Figure 1. Epicenter of the 23 June 2001 Earthquake

1. INTRODUCTION

The present study examines Peru's geologic and seismic complexity and the possible impact oblique subducting fractures zones - such as the Mendana (MFZ) to the North and the Nazca Ridge to the South – can have on the tsunamigenic efficiency of large earthquakes. For reasons not well understood, this narrow zone in Peru is characterized by shallow large earthquakes that can generate destructive tsunamis of varied intensities. Specifically examined is the significance of Nazca Ridge's subduction and migration to the seismicity of Central/Southern Peru, using as a case study the great earthquake of 23 June 2001 and the destructive local tsunami that was generated. Although the near-field effects of this particular tsunami were severe, the far-field effects were insignificant. Only a small tsunami was observed or recorded at distant locations in the South and Central Pacific and in Japan. The following sections document the tectonic characteristics of this southern region of Peru, the earthquake's impact, the source mechanism of the tsunami, the near and far field effects, historical events in this region and an evaluation of the potential for future tsunamigenic earthquakes for this region.

2. THE EARTHQUAKE OF 23 JUNE 2001

The earthquake occurred at 2033 UTC (4:33 PM EDT, 3:33 PM local time) on Saturday, June 23, 2001. Various magnitude values were subsequently estimated, such as M_w=8.4 (Harvard CMT), M_w=8.3 (USGS), M_w=8.2 (Earthquake Information Center, Tokyo). Final assigned magnitude was M_w=8.4. The quake's epicenter was off the coast at 16.15S 73.40W (Fig. 2), just north of the coastal town of Ocoña in Southern Peru, approximately 375 miles (600 km) southeast of Lima and 120 miles (190 km) west of Arequipa.

Figure 2. The Earthquake and Tsunami affected the southern region of Peru from Arequipa to Tacna.

Focal Depth - The earthquake occurred along an area of high seismicity. Its focal depth was listed as shallow (less than 33 Km); however, because a large portion of the plate interface ruptured, it was difficult to estimate a single representative focal depth value, although the USGS Moment Tensor Solution gave a depth of only 9 km.

Major Aftershocks - The quake ruptured the Nazca-South American plate inter-phase and was subsequently followed by several large aftershocks, which were visible on the GPS times (Melbourne et al., 2002). Following the main quake, more than thirty significant aftershocks ($M_w > 4.0$) occurred through 7 July 2001 with the largest having a magnitude of 7.6 on July 7 (USGS 2001). Figure 3 shows the epicenter and the extent of aftershocks over that period following the main shock. Periodic aftershocks continued in subsequent days, weeks and months.

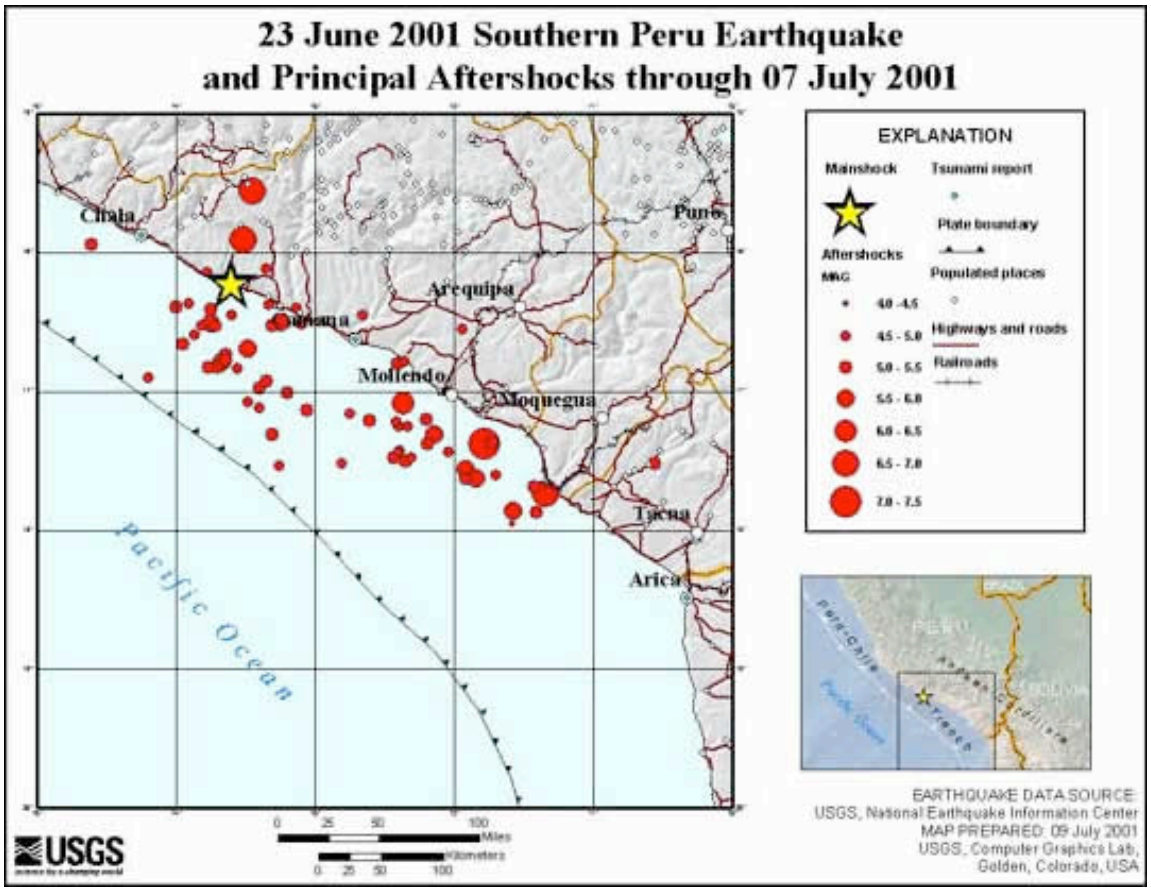

Figure 3. USGS Map of major Aftershocks through 7 July 2001

Focal Mechanism - The quake had a predominantly lateral strike slip with a smaller component of vertical dip slip motion. Figure 4 shows the determination of the earthquakes' focal mechanisms. Conventional magnitude estimates for this event ranged from M_s 8.2 to mantle magnitude M_m 8.6 (Okal and Talandier, 1989) – the latter corresponding to a seismic moment $M_0 = 4 \times 10^{28}$ dyn-cm. Other estimates of the seismic moment ranged from 1.2 to 4.9 $\times$ 10^{28} dyn-cm. The final Harvard determination, based on more data, gave the quake's strike at 310, the dip as 18, the slip as 63 and the energy release at 4.67 x 10^{28} dyn-cm.

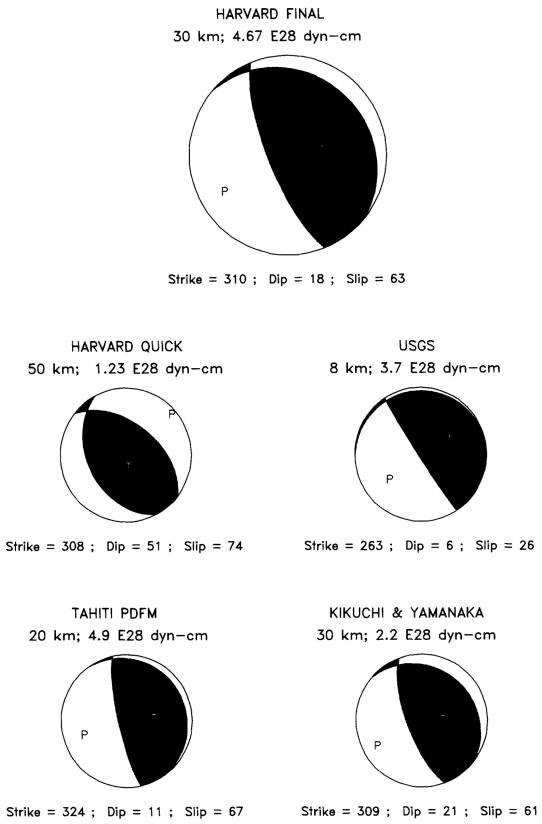

Figure 4. Focal Mechanisms as determined by Harvard, USGS, Tahiti PDFM and by Kikuchi & Yamanaka, 2001 (Univ. of Tokyo).

2.1 Earthquake Rupture

As stated, the 23 June 2001 earthquake ruptured a segment of the plate boundary between the Pacific and Nazca Plates. The rupture process may be linked to initial arc-parallel stresses caused by the bend in the South American subduction zone in this region and/or subduction of the Nazca Ridge (Macharé and Ortlieb, 1992). The initial rupture continued for about 70 km before encountering a 6,000 sq. km. area of the fault, which acted as temporary unbroken barrier for about 30 seconds. After this short interruption, the rupture front continued through this barrier at a low speed, slip and density of aftershocks, then for an estimated 200 km from the epicenter. The brief interruption of the rupture by the barrier was attributed to the regionally subducting fracture zone (Robinson et al. 2006). Similarly, based on broadband far-field seismograms with appropriate filters, parameterized and modeled the fault. The best fit solution of the model indicated that the rupture propagated in a southward direction at a very low speed of 1.6 km/sec with 80% of the final moment released as one patch 80 seconds after the onset of the rupture (Sladen et al., 2004). The significance of the subducting fracture zone, and the quake's slow rupture anomaly to tsunami generation is discussed in a subsequent section.

2.2 Earthquake Effects

The quake produced strong ground shaking that was felt in both southern Peru and northern Chile. Strong ground motions were also felt in many cities as far as Bolivia and Northern Chile. Even in Peru's capital, Lima (600 km away), homes collapsed, injuring several people.

According to reports, the ground motions in the affected region lasted for more than a minute. There was extensive destruction in southern Peru, particularly in the provinces of Arequipa, Moquegua and Tacna – where the highest intensities were observed (Fig. 5). In Arequipa and Moquegua, 80% of the homes were damaged as well as highways, water aqua-ducts and electrical systems. At the historic city of Arequipa (Fig. 6), Peru's second largest city with population of over one million people about 465 miles south of Lima, the quake destroyed historic homes and cathedrals, many of which had been rebuilt after the destructive 1868 earthquake. There were at least 73 reported fatalities in this area.

Figure 5. Region of Southern Peru mostly affected by the earthquake and tsunami of 23 June 2001.

In the southern city of Tacna, near the border with Chile, dozens of adobe homes were destroyed. Major damage occurred also in the zone known as La Yarada, where the electrical system was affected. There was extensive damage to the irrigation aqua-ducts in the valleys of Sama, Locumba and Tacna. Thirteen (13) people were reported killed in Tacna, and 8 in Ayacucho. Moquequa, a mining town about 1400 kms (865 miles) south of Lima, was also hard-hit. A landslide blocked one of the town's chief roads and many houses collapsed. Twenty-four people were reported killed and many more were injured. The Andean highland town of Characato was extensively damaged.

The quake practically wiped out the agricultural infrastructure of the region by causing the destruction of water reservoirs, canals and bridges. At Santa Rita de Sigua, the principal irrigation canal in this agricultural region, collapsed for about 300 meters - closing also the Pan-American Highway.

The number of dead, injured and missing continued to rise in the days following the main earthquake. According to Peru's Civil Defense Institute, as of June 26, 2001, 118 people had been killed, another 1,578 were injured, 53 were unaccounted and 47,696 were left homeless. A total of 21,189 homes were damaged or completely destroyed.

Figure 6. Extensive earthquake damage at Arequipa

2.2 Recent Earthquake Disasters in Peru

Destructive earthquakes occur with frequency throughout Peru. Prior to the 23 June 2001 event, the last major earthquake (7.7 magnitude) to strike along the Nazca subduction zone occurred on November 12, 1996. It killed 17 and injured about 1,500 people. On May 30, 1990, an earthquake (6.3 magnitude) in northern Peru killed 137 people. On May 31, 1970 another major earthquake (7.7 magnitude) killed approximately 70,000 people. On October 17, 1966, a strong earthquake (7.5 magnitude) off the coast of Pativilca severely damaged Central Peru. Also, this event generated a tsunami, which caused destruction along a 400 Km long coastal belt, from Chimbote in the North to San Juan in the South - including sectors of Lima-Callao (Pararas-Carayannis 1968, 1974). The USGS map below (Fig. 7) shows the epicenter of the 23 June 2001 earthquake, as well as the epicenters of major earthquakes to strike the region of Peru extending from 10^0 to 22^0 South Latitude.

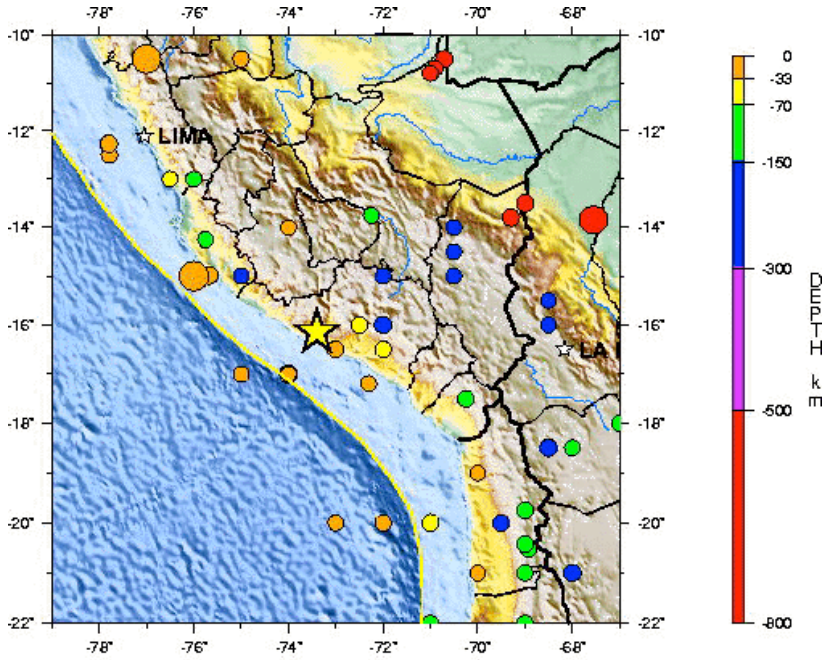

Figure 7. Epicenter of the 23 June 2001 Earthquake. Major Earthquakes since 1900 (USGS map)

3. THE TSUNAMI OF JUNE 23, 2001 IN SOUTHERN PERU

The June 23, 2001 earthquake generated a destructive, local tsunami, which struck the coastline, primarily near the epicenter region in southern Peru, approximately 20 minutes after the main shock. Based on the earthquake's large magnitude, initial visual reports and recordings from tide gauges in the region, the Pacific Tsunami Warning Center in Honolulu issued a Regional Tsunami Warning and Watch for Peru, Chile, Ecuador, Colombia, Panama, Nicaragua, El Salvador, Mexico and French Polynesia.

3.1 Near-Field Tsunami Impact

There were conflicting eyewitness reports as to the number of waves responsible for most of the damage in the area. It was reported that three to five separate waves struck and that either the second or third wave was the largest. Near-field damage was limited along the coastline from the town of Atico in the north, to Matarani in the south. Tsunami waves with run-ups ranging from 3 to 4.6 meters (10-15 feet) or more were reported. In some coastal areas, the tsunami waves swept one to two miles inland. Maximum tsunami run-up heights occurred along the coastlines of Chala-Camaná.

Camaná, a popular and picturesque summer resort of around 20,000 some 900 km (560 miles) south of Lima, was one of the hardest-hit areas by both the earthquake and the tsunami. The tsunami swept more than 800 meters (half-mile) inland over the town and its surrounding rice and sugarcane

fields. According to reports, 2,500 hectares of agricultural land were flooded. Maximum reported run-up exceeded 7 meters in some locations in the same area with greater than one-kilometer inland inundation. Eyewitness accounts from Camaná, described that four waves were responsible for most of the deaths and damage, the largest being the third. According to Peru's Civil Defense, at least 20 persons were reported drowned by the tsunami and another 60 persons as missing in this area.

La Punta, another popular resort area located along a narrow strip of beach immediately south of Camaná was also struck by powerful tsunami waves, which destroyed hundreds of homes, hotels and restaurants. Fortunately the tsunami struck when it was still wintertime in the southern hemisphere and beachfront communities were mostly deserted. The tsunami there was responsible for about 26 deaths with another 70 more reported missing in this area.

3.2 Far-Field Tsunami Effects

According to the Pacific Tsunami Warning Center's Bulletin in Honolulu, the following initial tsunami wave measurements (peak to trough) were reported from tide stations in Peru, Chile and the Galapagos (Table 1).

Table 1. Initial Tsunami Wave Recorded in Peru, Chile and the Galapagos

Tide Gauge Station	Measurement (Peak to through in m.	Wave Period (min.)
CALLAO (Peru)	0.4	14
SANTA CRUZ (Galapagos)	0.6	16
ARICA (Chile)	2.5	15
IQUIQUE (Chile)	1.5	20
ANTOFAGASTA (Chile)	0.9	18
CALDERA (Chile)	1.0	16
JUAN FERNANDEZ (Chile)	0.8	10
VALPARAISO (Chile)	0.5	18
SAN ANTONIO (Chile)	0.4	18
COQUIMBO (Chile)	1.0	18
CORRAL (Chile)	0.3	18
TALCAHUANO (Chile)	1.0	16
SAN ANTONIO (Chile)	0.3	15

The tsunami was observed or recorded by tide gauges across the Pacific Ocean. Small waves measuring a few centimeters were recorded or observed in the Southern and Central Pacific and as far away as Hawaii and Japan. The greatest tsunami oscillation of 30 cm peak to trough was recorded at Port Vila, Vanuatu, in the Southern Pacific. Additional tide gauges in the Central and South Pacific (Apia, Fanfuti, Kembla, Lautoka, Lombrum, Nukualofa, Rarotonga and Suva) recorded a small tsunami.

In Honolulu, Hawaii, a small influx of the tsunami was observed in the Kapalama and Nuuanu Streams, beginning at approximately 00:30 hours of June 24th. The observed water movements had an apparent period of 15-20 minutes.

3.3 Large Historical Tsunamis from Peru Earthquakes

Large tsunamigenic earthquakes occur frequently in Peru. The historic record shows that major earthquakes occurred on 9 July 1586, 13 November 1655, 20 October 1687, 28 October 1746, 30 March 1828, 24 May 1940 (M=8.4), 17 October 1966 (M= 7.5), 31 May 1970 (M= 7.7), 3O May 1990 (M=6.3) and 12 November 1996 (M=7.7). Of these, the earthquakes of 1586, 1687, 1746, 1828 and 1966 produced destructive tsunamis (Iida, Cox and Pararas-Carayannis, 1968; Pararas-Carayannis, 1968, 1974). To this list we must now add the June 23, 2001 event.

The 1868 Pacific-wide tsunami, characterized as the "Great Peru earthquake and tsunami", which destroyed Arica (then part of Peru), had its epicenter further south - in what is now northern Chile (around 18.5^0 South). The last major tsunami to strike Peru was on October 17, 1966. It affected a coastal belt 400 Km long, causing destruction from Chimbote in the North to San Juan in the South. The greatest wave at Callao had a range of 3.40 m height (range between maximum crest and trough) and tsunami waves exceeding 3 meters in amplitude (height above undisturbed water level) inundated La Punta, Chuito, Ancon, Huaura, Huacho, and the resort of Buenos Aires in the City of Trujillo. Devastating effects were experienced at the port of Casma (about 360 Km north of Lima) and at Calota Tortuga, where waves exceeded 6 meters in range. Tsunami destruction also occurred at Puerto Chimu and Culebras. The 1966 tsunami caused no damage outside Peru, but was recorded by tide gauges throughout the Pacific Ocean (Pararas-Carayannis, 1968, 1974).

3.4 Tsunami Generating Area

The azimuthal orientation of a tsunamigenic area can be estimated from seismic and oceanographic data, as well as from the distribution of major aftershocks immediately following the main quake (Pararas-Carayannis, 1965, 1968, 1972, 1974). The nature of the first seismic motion related to an earthquake depends on the crustal displacement at the source. The impulse of P (compression) waves indicates a vibration in a plane containing the great circle that passes through the epicenter and the seismic station recording the earthquake (Galitzin, 1909). If the first impulse on the vertical component of the seismograph is up, the first phase of P wave is a compression, so the composition of north south and east west is in a direction away from the epicenter. A composition of the three components gives the direction of the first displacement of the ground, which however is not the exact direction of the path of the incident wave. It is rather the combination of the amplitudes of the incident P wave and the reflected P and S (shear) waves that give an indication of the motion of the surface of the ground at the source. These are significant parameters in understanding the tsunami source mechanism. This understanding has greatly improved with the use of data from broadband seismometers.

Although these are basic concepts, it may be helpful to summarize them. In brief, a single force

sends compression waves into a half space and rarefaction waves into the other half space; a couple sends alternate compressions and rarefactions into quarter spaces (Nakano, 1923). Modal planes of the focus can be deduced from recordings of compressions and rarefactions (Byerly, 1955). Such a pattern can be considered a function of the azimuth to be expected from a seismic source. From this and the distribution of aftershocks, the tsunamigenic area can be approximated.

Additionally, the tsunamigenic area of an earthquake can be deduced indirectly from oceanographic parameters by refracting tsunami waves back to the source from tide gauge stations, which recorded the tsunami, and for a length of time equal to the travel time to each station. Using several stations and based on water wave refraction analysis, an approximate envelop can be established giving the approximate orientation and dimensions of the tsunamigenic area (Pararas-Carayannis, 1965, 1972, 1974).

Review of aftershock distribution following the June 23, 2001 earthquake main shock and analysis of the moment tensor, indicated initially that the fault rupture and the tsunamigenic area (an approximate ellipse), had a general trend striking at 284 degrees with a dip=7 and a slip 45. However, and as indicated previously, the final Harvard determination gave the quake's strike at 310^0, the dip as 18, and the slip as 63. The distribution of aftershocks at sea had a similar azimuthally NW-SE distribution paralleling the Peru coastline, thus defining the tsunami generating area as approximated in Fig. 8.

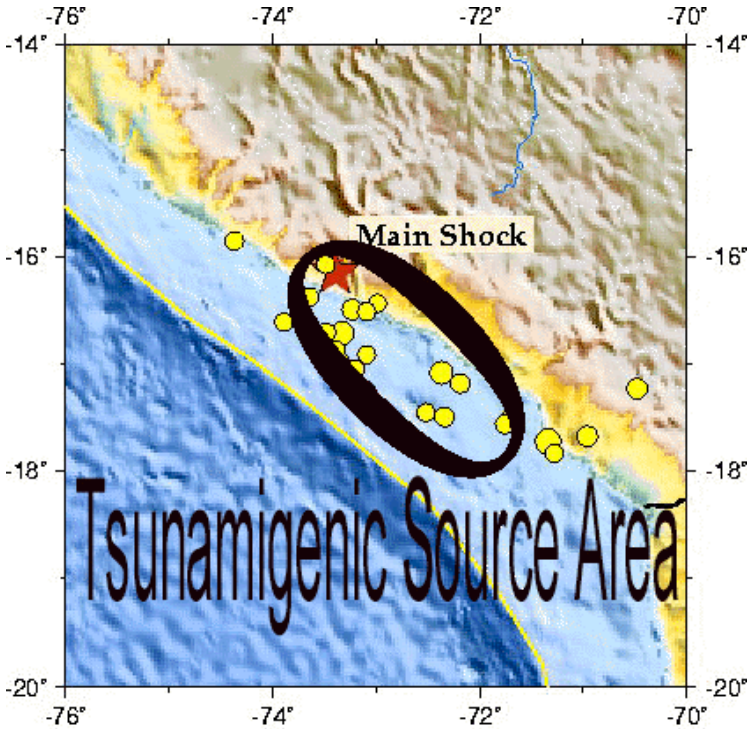

Fig. 8 The Generating Area of the 23 June 2001 tsunami.

The azimuthal orientation of the tsunami generating area shown in this map is in agreement with the general trend of the fault systems, the Andean Mountains, and the Peru-Chile Trench in this region.

The dimensions of the tsunami generating area given in the literature varied depending on the use of the seismic inversion of the rupture process that was used. For example, by using a shallow-dipping nodal plane consistent with an inter-plate thrust earthquake along the Peru subduction zone and assuming a magnitude of only Mw=8.2, the moment distribution showed a rupture area that was 210 km long and 120 km wide (Kikuchi and Yamanaka, 2001). However, according to other studies discussed earlier (Macharé and Ortlieb, 1992), the initial rupture of the 2001 earthquake was 70 km before encountering a 6,000 sq. km. area of the fault, which acted as a temporary unbroken barrier for about 30 seconds. As indicated, after this short interruption and possible stress transference, the rupture front of perhaps a different event continued in a southeasterly direction through this barrier on another segment for another 200 km. Therefore, the combined tsunami generating areas of perhaps two distinct events - separated in time by 30 seconds - must have been at least 300 km long and perhaps wider than 210 km. These dimensions of the tsunami generating area are also supported by the aftershock distribution and the rupture, which extended southeast from the epicenter to the vicinity of Ilo, about 150 km north of the Chilean border. Based on the estimated fault length, the tsunami generating area is roughly calculated to cover about 17,200 sq. km.

3.5 Ocean Floor Displacements and Initial Tsunami Height

Dynamic motions during the earthquake and co-seismic vertical displacements provided the initial conditions for tsunami generation and propagation. However, since the earthquake's rupture area extended landward of the coastline, only a part of the co-seismic deformation contributed to tsunami generation. These crustal displacements were of a dipole nature (negative and positive) along a thrust fault approximately paralleling the Peruvian coast. The co-seismic vertical displacements probably varied along the different segments along the rift. The maximum vertical uplifted movement is estimated to have been about 1.8 m on the continental side of the rift and about 1.8 downward on the oceanic side of the rift. However, these represent maximum crustal displacement values diminishing away from the rift zone. Upward, ground displacements also occurred on land along the affected coastal area, as well as other significant co-seismic lateral movements, which may have disturbed sedimentary layers of the accretionary prism, thus contributing also to the tsunami height.

Since the June 23, 2001 earthquake in Peru was very shallow in depth (9 km), this may have limited the extent of the displacements and thus the tsunamigenic area. The quake had a predominantly lateral strike slip with a smaller component of vertical dip slip motion. It is the latter motion that contributes significantly to tsunami generation. Based on empirical relationships we can estimate the total displacement which is the resultant of the horizontal strike slip, "X", and the vertical dip-slip, Z, related by:

Total Displacement = $X^2 + z^2$ (raised to ½)

The horizontal strike slip and the vertical dip slip for this event are not known with certainty - although the maximum vertical crustal displacement is estimated at 1.8 meters. However, statistical relationships between maximum crustal displacement and earthquake magnitude M were

compiled in the past and working curves have been plotted (Wilson 1964, 1969). Although such empirically derived curves display scatter of data - possibly because of differences in the focal depth and geology of each region associated with each seismic event - a median value can be selected as being reasonable for shallow-focus tsunamigenic earthquakes. For the June 23, 2001 earthquake (Mw = 8.4), the median value of crustal displacement along the fault taken from such curve is 5.4m. These were the estimated co-seismic displacements and offsets. However, GPS data collected subsequently over a two-year period, indicated additional post-seismic offsets and deformation, which were slowly decreasing. The observed co-seismic subsidence was followed by post-seismic vertical uplift and slow aseismic westward movement of the Peruvian coastline (Melbourne et al, 2002, Perfettini et al, 2005). Of course such post-seismic deformation does not contribute to tsunami generation.

If we assume an extreme ratio of strike-slip: Dip-slip, 10:3, then dip-slip, or vertical movement of the ocean floor along the fault, is estimated from the equation above to be, Z = 1.78m. Preliminary source inversions for the main shock indicated thrust slip ranging from 1 to 8 meters over a broad asperity that was 200 km by 300 km centered to the southwest of Arequipa (Kikuchi and Yamanaga, 2001). However, this occurred mainly over a land area and not in the ocean.

Long ago it was established that vertical displacements of a seismotectonic block responsible for tsunami generation will decay exponentially with distance normal to the fault in accordance to the elastic rebound theory (Reid 1910). Thus, the ocean area affected by such displacements - the tsunami generating area - is an approximate ellipse in which the fault occupies the major axis, which possibly coincides with the rupture zone if it is located in the ocean. The leading tsunami waves are generated from the periphery of this area - and their arrival at nearby stations – is also indicative of the initial ocean floor displacement. Maximum run-up on the shore, is generally caused by the crest of the tsunami wave near the fault.

Based on the above assumptions of vertical ocean floor displacements, the initial tsunami height in the generating area is estimated at a maximum of 1.5 - 1.78 meters above the undisturbed sea level. Given, therefore, the magnitude, depth and epicenter of the earthquake and utilizing the assumptions and empirical relationships outlined here, the run-up along Southern Peru from tsunamis originating from this seismic region can be roughly approximated. Considering that the measured waves reaching the immediate coastline of Southern Peru had maximum run-ups of about 5 meters, the shoaling and resonance amplification factor on this coast for local tsunamis is estimated to be about 2.8 times the maximum deep water value (1.78 x 2.8 = 4.99 meters).

As stated, the earthquake's focal mechanism indicates that the tsunami was generated from dipole type of crustal movements, which involved vertical displacements. However, the earthquake also involved lateral movements, which must have affected the sediment layers in the accretionary prism on the landward side of the fault. Such lateral compression of sediment layers probably resulted in up-thrusts in this zone, which contributed to the formation and destructiveness of the tsunami locally.

3.6 Fault Length

Statistical relationships between fault length L (Km) and earthquake magnitude (M) have been also worked out in the past. Using such a statistical relationship as documented in the literature

(Ambraseys and Zatopek, 1968), we can estimate the fault length to be:

$$\text{Log } L = 1.13\ M - 6.4$$

If we assume that the earthquake of June 23, 2001 had the equivalent Richter magnitude of 8.1, the fault length estimated by such early empirical relationships would be only about 152 km. However since such empirical relationships relate to Richter magnitude and not to Moment Magnitude (estimated at Mw=8.4) they do not provide a reliable estimate. As stated, seismic inversion of the rupture process indicated that the actual fault length for this event was much longer. The fault was at least 300 km long. The width of the affected area was as much as 210 km or more.

4.5 Tsunami Energy

The 2001 Peru earthquake (Mw =8.4) released the largest moment of any event in the previous 30 years and produced over 50 cm of co-seismic offset at the GPS tracking station at Arequipa (AREQ), which is located about 100 km from the coast (Melbourne et al., 2002). Based on the estimated fault length, the tsunami generating area is roughly calculated to cover about 17,200 sq. km. According to the final Harvard tensor analysis, the energy release of the earthquake was 4.67×10^{28} dyn-cm. The energy that went into tsunami generation can be estimated on the basis of the source dimensions and the energy that resulted in the uplift or depression of the ocean floor. Assuming that the total energy is equal to the potential energy of the uplifted or depressed volume of water, the total energy for the tsunami can be roughly approximated by:

$$(E_t) = 1/6\ p.g.h^2$$

Where E_t = Total energy

p = 1.03 g/cm = Density of sea water

g = 980 cm/sec = gravitational acceleration

h = Assumed average height of crustal displacement (throughout the tsunamigenic area) = .55 m

Since the Tsunami generating area (A) is 17,200 Km, the energy of the tsunami can be estimated to be

$$E = 1/6\ p.g.h^2.A = 1/6(1.03)(.980)(10^3)(10^4)(.55^2)(17{,}200 \text{ sq. km}) = 8.99 \times 10^{19} \text{ ergs (or dyn-cm).}$$

where 1 erg = g cm sec.

Considering that the energy of the June 23, 2001 earthquake (M_w 8.4) was very large, the energy

responsible for tsunami generation was a small fraction of the total earthquake energy, which – according to the Harvard final estimate was as much as 4.67 x 10^{28} dyn-cm.

5. DISCUSSION

As illustrated by Fig. 9, Central and Southern Peru is a region of high seismicity caused by active interactions of major tectonic plates as well as oblique subduction of migrating oceanic ridges, which influence the size and depth of coastal earthquakes and the generation of tsunamis. The following sections review the significance of such interactive processes to tsunami generation. Although the discussion pertains to Central/Southern Peru using primarily the 23 June 2001 tsunami as a case study, the analysis is also applicable to other areas where oceanic ridges subduct obliquely under continents, as for example along the North America continent, along Chile and elsewhere.

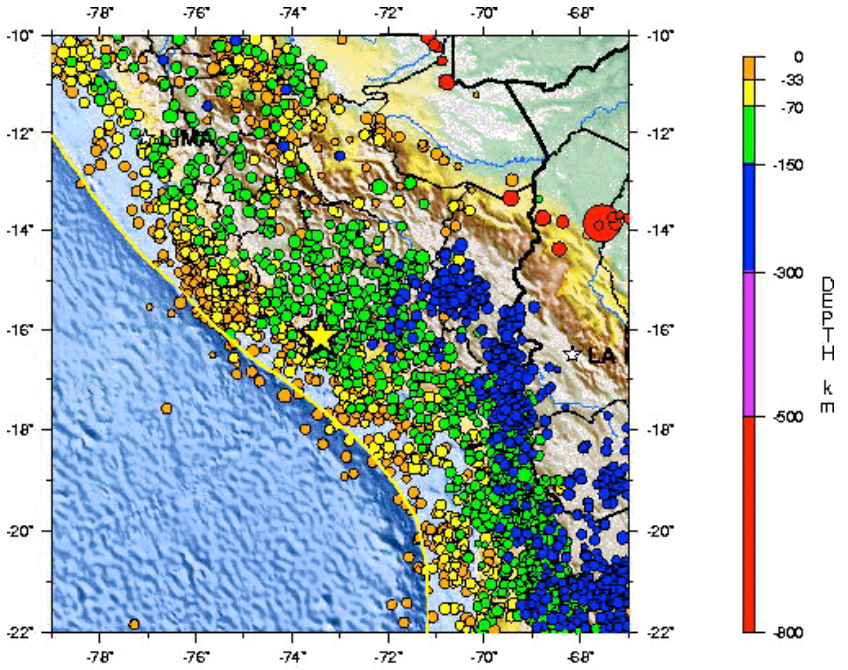

Fig. 9 Epicenter of the June 23, 2001 Earthquake / Seismicity of Southern Peru (USGS graphic)

5.1 Significance of Nazca Ridge's Oblique Subduction and Migration to the Seismicity of Central/Southern Peru and to Tsunami Generation

Southern Peru is a region of considerable geologic and seismic complexity because of the obliquity of converging tectonic plates at about 77 mm per year. However, the angle of subduction of the Nazca oceanic plate beneath the South American plate is not uniform along the entire segment of the Peru-Chile Trench fronting Peru. Furthermore the angle of subduction is apparently affected by buoyancy

forces of the bounding oceanic ridges and fractures - such as the Mendana Fracture Zone (MFZ) to the North and the Nazca Ridge to the South in Northern/Central Peru, as previously documented (Pararas-Carayannis, 2007; Sacks, 1983).

The overall subduction in the Peru segment of the Trench begins with a dip of about 30 degrees. However, seismic reflections studies indicate that it then flattens out and becomes sub-horizontal between 100 and 150 km depth beneath Peru, before steepening and descending into the earth's mantle. Also, seismic studies indicate that the flat slab segment exhibits a 20-40 km lithospheric "sag", approximately mid way between relative highs from 5^0 to 13^0 South. This suggests a double buoyant plateau model, with the Nazca Plate supported by two light bodies - the Mendana Fracture Zone (MFZ) to the North and the Nazca Ridge to the South. Such "saging" due to buoyancy forces would be expected to affect the source mechanisms of earthquakes, particularly near areas where an oceanic ridge, such as the Nazca Ridge, intercepts the continent. In fact the epicenter of the earthquake of August 15, 2007 was near this "sag" at 13.353^0 S, very close to the region of Nazca Ridge convergence with the South American continent. However, the 23 June 2001 earthquake was at 16.15^0S, 73.40^0W, south of Nazca Ridge's subduction zone, near a geologically anomalous, syntaxial region of Peru where there is a higher density of shallow earthquakes and a change in the obliquity of tectonic subduction (Fig. 10).

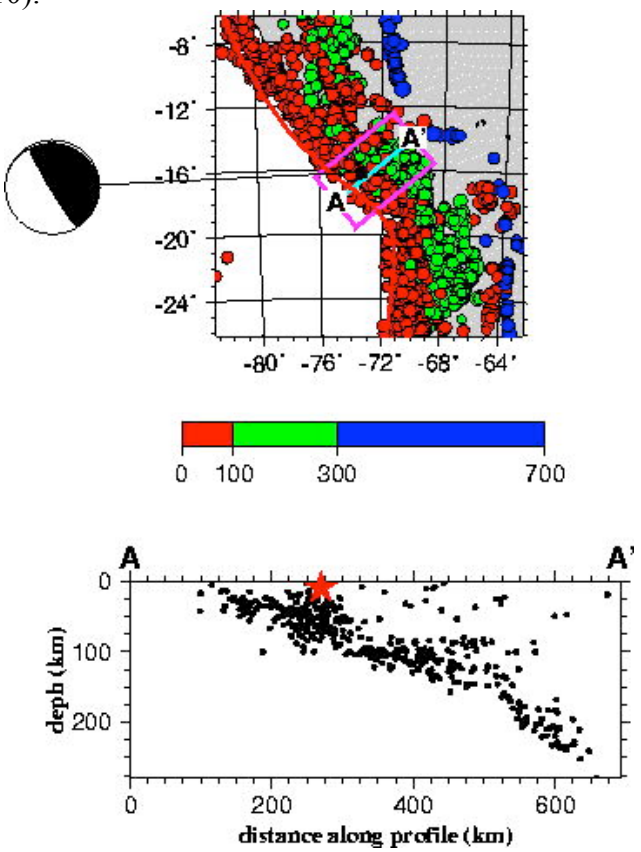

Figure 10. Focal mechanism of the 23 June 2001 Earthquake. Distribution of the foci of intermediate and deeper earthquakes underneath the continent in the South Peru region (Internet graphic)

5.2 Examination of Seismic Anomalies and Possible Effects on Tsunami Generation

Let us examine further the Nazca Ridge and what causes the observed seismic anomalies near the region where the 23 June 2001 tsunami was generated. The Ridge originated at the Easter Island hotspot. Review the Ridge's subduction process beneath the South American continent indicates that it is oblique and occurs from about 13.5^0 to 15.6^0 South and has been responsible for varying uplift rates and extensive crustal deformation of the upper plate from the northeast to southwest along the Peruvian coast during the Quaternary and thereafter (Pararas-Carayannis, 2007). The Ridge's varying rates of convergence and oblique northeastward orientation relative to the east-west direction of plate convergence has resulted in an approximate 70 mm/yr southeastward migration of the zone of the Ridge's subduction beneath the Peruvian coast. This is evident by a narrowing of the shelf, a westward shift of the coastline and the presence of marine terraces.

Above the southern flank of the Nazca Ridge, the coast is still rising at a fast rate as determined from studies of marine terraces on the coasts of Peru and Chile (Hsu, 1992; Hampel, 2002). The pattern of faster uplift above the southern flank and the slower uplift above the northern flank of the Ridge is a predictable consequence of the Ridge's oblique subduction. However, this has created anomalies which affect also the seismicity of the region on both sides of the Nazca Ridge's subduction zone and has created asperities which limit the length of earthquake ruptures, the depth of quakes, as well the tsunami generating sources and processes. The 23 June 2001 earthquake's epicenter at 16.15^0 was just south of the Ridge's southern flank and north of the generating area where the great 1868 Arica tsunami was generated. Thus, the 2001 event did not have as great of a rupture zone as that of 1868.

In addition to seismic reflection studies, review of studies of mineral concentrations provides additional clues for geotectonic anomalies that can also help determine whether a destructive tsunami may be generated along a specific segment of the active marginal convergence zone in Southern Peru. Magmatic-hydrothermal ore deposit concentrations were found in regions of Peru associated with aseismic ridge subduction (Fig. 11).

Specifically, magmatic-hydrothermal ore deposits found in the Andes and along certain coastal regions of Peru have been correlated to past distinct and sudden metallogenetic episodes during the last 200 Ma - episodes not necessarily associated with the progressive eastward movement of the Nazca plate beneath the continental South American plate (Rosenbaum et al. 2005 A, B).

The localized concentrations of ore deposits suggest the existence of crustal heterogeneities within the subducting oceanic plate (the Nazca plate) - which are particularly prevalent in the Southern Central Peru region. These heterogeneities may be caused by the suspected crustal buoyancy anomalies, which affect the dynamics of the subduction system in this particular region of Peru (near the Nazca Ridge in central Peru where the August 15, 2007 earthquake occurred). Accordingly, there may be laterally migrating zones of flat ridge subduction which could account why the great M_W+8.1 magnitude earthquake of 15 August 2007 did not generate a tsunami of great far-field significance as other earthquakes further north or further south have done (Pararas-Carayannis, 2007).

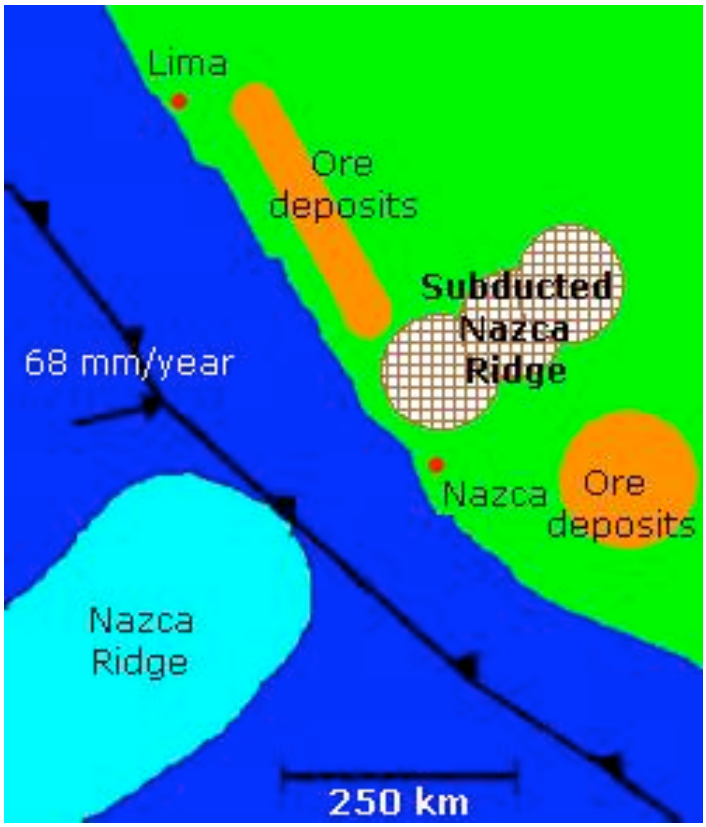

Fig. 11. Localized concentrations of ore deposits suggesting the existence of crustal heterogeneities within the subducting oceanic plate (After Rosenbaum et al. 2005 A, B)

5.3 Examination of the Earthquake Rupture Effects on Tsunami Generation

Let us further examine the tectonic geometries of Central and Southern Peru and the implications of Nazca Ridge's subduction to seismic anomalies that can affect tsunami generation. Specifically, in the vicinity of the Nazca Ridge intersection with the South American continent, it appears that there is a northward kink in the subducting extension - which would also support the existence of different tectonic geometry by northward-trending lateral compressive forces - the same forces that have formed the Paracas peninsula ending at Punta Huacos. Thus, the length of earthquake-caused ruptures in this region is limited. This is a reasonable explanation why the earthquake of 15 August 2007 in the region did not generate a destructive tsunami elsewhere except in the immediate region (Pararas-Carayannis, 2007). As stated, apparent changes in the geometry of subduction of the Nazca Ridge as well as heterogeneous compressive forces affect tsunami generating mechanisms along Central and Southern Peru by limiting the extent of earthquake ruptures and areas of crustal displacements. This holds true for many other areas where similar oceanic ridges intersect continents. Figure 12 illustrates the evolution of tectonic anomalies by the compressive forces generated by the subduction of Nazca Ridge and migration.

From this preliminary analysis we can reasonably conclude that earthquakes further north and south of the Nazca Ridge have the potential of generating local destructive tsunamis in Peru with more extensive far-field impact. However earthquakes that occur in the region near the Nazca Ridge intersection appear to have shorter ruptures and a diminished potential for far-field destructive tsunamis.

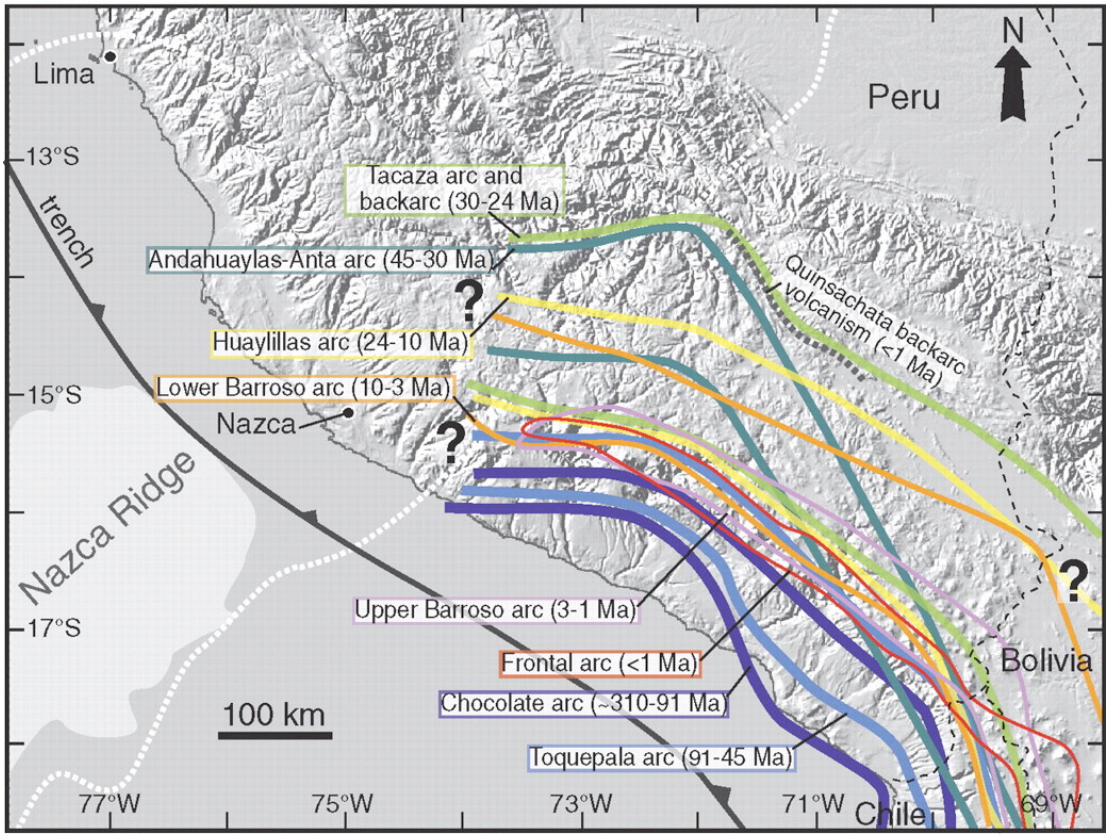

Figure 12. Evolution of tectonic anomalies in Southern Peru generated by compressive forces of Nazca Ridge's subduction and migration (Internet graphic).

Further review of earthquake rupture processes for this southern region of Peru indicates that they are apparently linked to initial arc-parallel stresses caused by the bend in the South American subduction zone and/or the subduction of the Nazca Ridge and on other anomalous structures. These structures appear to also limit the length of ruptures and of their speeds, thus limiting also the size of a tsunami's generation area and its source parameters. This limitation is particularly significant in that tsunamis that are generated in the segment ranging from about 16^0 to 18^0 South Latitude, can be destructive locally but do not seem pose a threat for the rest of the Pacific. This is also supported by the historical records of tsunamis described earlier (Pararas-Carayannis, 2007).

5.4 Examination of Spatiotemporal Anomalies of the 23 June 2001 Earthquake and Effect on Tsunami Generation

There is a noticeable higher density of shallow earthquakes near the subduction zone of the Nazca Ridge (Fig. 12). Apparently, events in this central/southern region of Peru are controlled by local tectonic anomalies. For example, the great earthquake of 23 June 2001 in the region was anomalous since it involved spatiotemporal slip distributions that differed significantly from the predominantly unilateral or bilateral rupture expansion that is typical for other great earthquakes elsewhere (Lay et al, 2010). As documented in the literature (Macharé and Ortlieb, 1992), the initial rupture of the 2001 earthquake continued for about 70 km before encountering a 6,000 sq. km. area of the fault which acted as a temporary unbroken barrier for about 30 seconds. After this short temporal interruption, the rupture front continued in a southeasterly direction through this barrier, but at the rather low speed of 1.6 km/sec, for about 200 km. Finally, 80% of the final moment was released as one patch 80 seconds after the onset of the rupture (Sladen et al., 2004). As indicated, the brief interruption of the rupture by the barrier was attributed to the regionally subducting Nazca Ridge - fracture zone (Robinson et al. 2006). The slow rupture speed after the barrier, indicates the existence of sedimentary layers within an accretionary prism which, when up-thrusted by vertical as well as lateral crustal displacements, contributed significantly to a more efficient local tsunami generation.

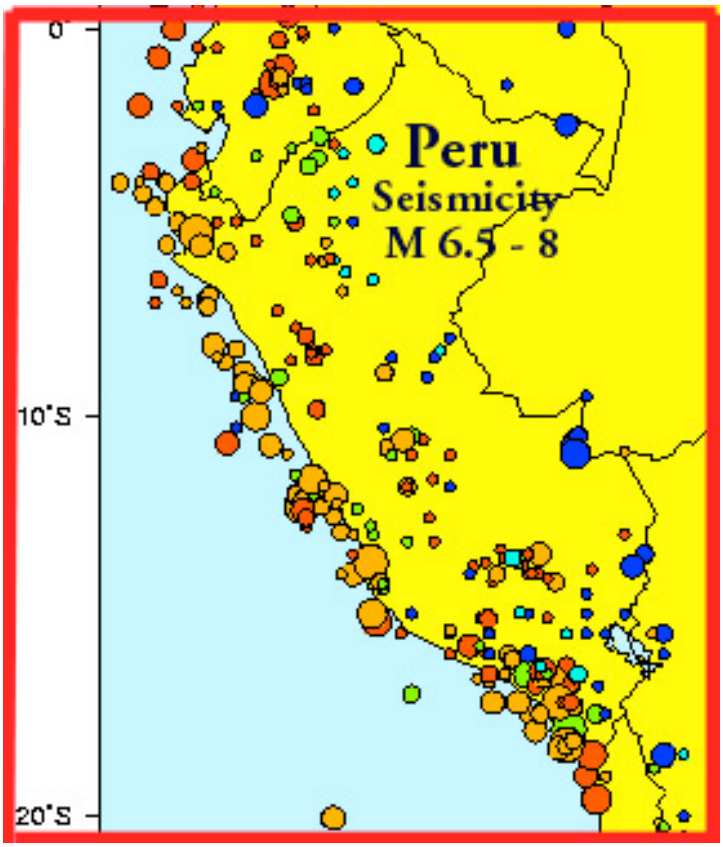

Figure 12. Seismicity of Peru (Magnitude 6.5 - 8) (Pararas-Carayannis, 2007)

5.5 Tsunamigenic Potential along Southern Peru

As documented, the Peru-Chile Trench is a manifestation of very active subduction along the South American continent. Most of the destructive tsunamis along the South American coast have been generated from major, shallow earthquakes, east but in close proximity to the Peru-Chile Trench. Deeper earthquakes along the Beniof Zone (which is quite wide and flat in this area of Southern Peru) do not produce tsunamis). Historically, the large earthquakes along the Peru-Chile Trench above latitude 16^0 South have produced locally destructive tsunamis but not destructive Pacific-wide tsunamis. For example, the 1966 tsunami which was generated by a large earthquake in the central part of Peru's seismic zone 4, had a rather short rupture of about 120 km (Pararas-Carayannis, 1968, 1974). It did not produce a Pacific-wide tsunami. Similarly, the June 23, 2001 Peru earthquake had a relatively short rupture (estimated at max. 300 km) and did not generate a large Pacific- wide tsunami.

The gradients in obliquity appear to change south of 18.5^0 as a consequence of the geometry of tectonic plate motions. In this region, the rupture lengths of major earthquakes are longer and the tsunamigenic potential is greater. The real destructive Pacific-wide tsunamis have been generated along the coast of Chile. The 1868 Pacific wide tsunami, characterized as the "Great Peru earthquake and tsunami", which destroyed Arica (then part of Peru), had its epicenter further south - in what is now northern Chile (around 18.5^0 South).

The May 9, 1877 (Mw 8.8) quake near Iquique, had a rupture of about 420 km along the coast of Chile and extended from 18^0 to 23^0 South latitude and generated a destructive Pacific-wide tsunami. The wave heights of that event reached 24 meters in Chile and up to 5 meters in Hawaii (Pararas-Carayannis 1969; Pararas-Carayannis and Calebaugh, 1977).

The November 10, 1922 earthquake (M_t 8.7) in Northern Chile, had a rupture of about 300-450 km-long, extending from about 26.1^0 to 29.6^0 South. It generated also a Pacific-wide tsunami - although not as large as that generated by the 1877 or 1868 earthquakes. Finally, the 1960 Pacific-wide tsunami was generated by another great earthquake which had its epicenter at about 37.5^0 South. The reason this tsunami was so destructive in Hawaii, Japan and elsewhere in the Pacific, was that the 1960 earthquake's rupture extended along a strike length of about 900 -1000 km.

More recently, the great (M_w=8.8) earthquake of 27 February 2010 occurred along a segment of Chile's central seismic zone - extending from about 33ºS to 37ºS latitude, just south of the Juan Fernández ridge. Because of the proximity to the ridge, this earthquake also had a complicated rupture process and co-seismic displacements (Fig. 13). The total rupture was about 550 km long and extended to about 50 km in depth. This is also an area where active, oblique subduction of the Nazca tectonic plate below South America occurs at the high rate of up to 80 mm per year. The unusual rupturing process of the 2010 earthquake also released energy gradually, which could partially account for the less severe near and far-field tsunami effects. Apparently the geodynamics of the Juan Fernández ridge had an impact on this earthquake's rupture, crustal displacements and the generation of the tsunami (Pararas-Carayannis, 2010).

In conclusion, it appears that the obliquity of convergent tectonic plate boundaries and the subduction of oceanic ridges along southern Peru may be the reason for the shorter rupture lengths of earthquakes and the generation of only local destructive tsunamis. The historic record also supports such conclusion.

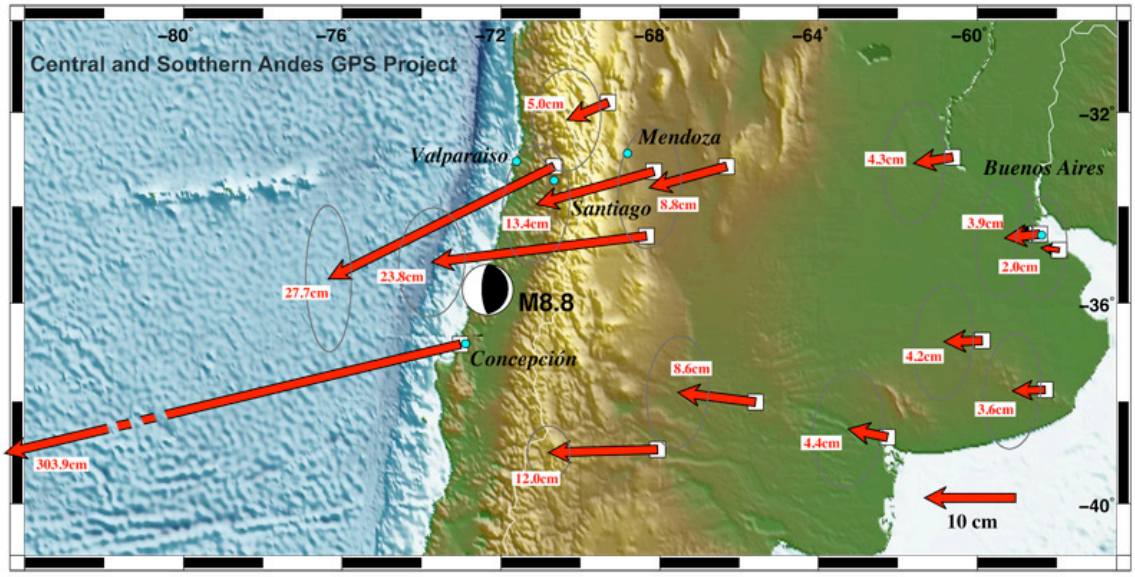

Fig. 13. Co-seismic displacement field associated with the February 27, 2010 Maule earthquake in south-central Chile, based on GPS Geodetic measurements (James Foster and Ben Brooks, University of Hawaii). Note proximity of the epicenter to the Juan Fernández ridge

5. SUMMARY AND CONCLUSIONS

The angle of subduction of the Nazca oceanic plate beneath the South American plate is not uniform along the entire length of the Peru-Chile Trench and particularly along the segment fronting Peru. Subduction along Peru is affected by buoyancy forces of the bounding oceanic ridges and fractures - such as the Mendana Fracture Zone (MFZ) to the North and the Nazca Ridge to the South – which create "saging" and anomalies which affect the source mechanisms of earthquakes.

The geodynamics of Nazca ridge in the vicinity of Central and Southern Peru involve oblique subduction and migration which is changing the geologic structure of the region. The Ridge's oblique subduction process beneath the South American continent occurs from about 13.5^0 to 15.6^0 South and has been responsible for varying uplift rates and extensive crustal deformation of the upper plate from the northeast to southwest along the Peruvian coast. The crustal buoyancy anomalies on both sides of the Nazca Ridge's subduction zone have affected also the seismicity of the region and have created asperities which limit the length of earthquake ruptures, as well as the tsunami generating sources and processes. Earthquakes near the Nazca Ridge intersection appear to have shorter ruptures and a diminished potential for far-field destructive tsunamis. This limitation is particularly significant for tsunamis generated along the segment ranging from about 16^0 to 18^0 South. The large tsunamigenic earthquakes of August 15, 2007 north of the Nazca Ridge and of 23 June 2001 to the south, are typical events that can be expected along the coasts of Central and South Peru. The local destructive tsunamis that were generated did not have any significant far-field impacts.

The gradients in obliquity appear to change south of 18.5^0 South as a consequence of the geometry of tectonic plate motions. In this region, the rupture lengths of major earthquakes are longer and the tsunamigenic potential for Pacific-wide impact, greater.

REFERENCES

Byerly, P., 1955. "Nature of Faulting as Deduced from Seismograms", Geol. Soc. Am. Spec. Paper 62, 75-86.

Fisher, R. L. and Raitt, W. R., 1962. "Topography and Structure of the Peru-Chile Trench", Deep Sea Res., 9, 423-443.

Galitzin, B.,1909. "Zur Frage der Bestimmung des Azimuts der Epizentrums eines Bebens"; Assoc. Internat. de Sismologie, C. R. Zermatt, 1909, pp. 132-141.

Gutenberg, B. and Richter, C. F., 1954. "Seismicity of the Earth" 2nd Edition, Princeton Univ. Press, Princeton, N.J., p. 310.

Gutenberg, B. and Richter, C., 1956. "Earthquake Magnitude, Intensity, Energy and Acceleration", 2, Bull. Seismol. Soc. Am., 46 (2), 105-143.

Hampel, A., 2002. The migration history of the Nazca Ridge along the Peruvian active margin: a re-evaluation. Earth and Planetary Science Letters.Volume 203, Issue 2, 30 October 2002, Pages 665–679
http://www.sciencedirect.com/science/article/pii/S0012821X02008592

Hsu, J.T., 1992. Quaternary uplift of the peuvian coast related to the subduction of the Nazca Ridge: 13.5 to 15.6 degrees south latitude. Quaternary International, Vol. 15-16, 1992, Pages 87-97.

Iida, K., D. Cox and G. Pararas-Carayannis, (1968). "Prelim. Catalogue of Tsunamis Occurring in the Pacific Ocean", Hawaii Institute of Geophysics, Univ. of Hawaii, Data Rept. No. 5.

Kikuchi, M. and Y. Yamanaga, 2001. Earthquake Information Center seismological note 105, Earthquake Information Center, Earthquake Research Institute, Univ. of Tokyo, 2001.

Lay, T., Ammon, C.J., Hutko, A.R. and H. Kanamori, 2010. Effects of Kinematic Constraints on Teleseismic Finite-Source Rupture Inversions: Great Peruvian Earthquakes of 23 June 2001 and 15 August 2007. Bulletin of the Seismological Society of America June 2010 v. 100 no. 3 p. 969-994.

Lomnitz, C., and Cabre' R. (1968). "The Peru Earthquake of October 17, 1966", Bull. Seism. Soc. Am., Vol. 58, No. 2, pp. 645-661, April.

Macharé and Ortlieb, 1992. Plio-Quaternary vertical motions and the subduction of the Nazca Ridge, central coast of Peru. Tectonophysics 205, 205, 97-108.

Melbourne, T. I., F. H. Webb, J.M. Stock, and C. Reigber, Rapid postseismic transients in subduction zones from continuous GPS, J. Geophys. Res., 107(B10), 2241, doi:10.1029/2001JB000555, 2002.

Nakano, H., 1923. Notes on the nature of the forces which give rise to the earthquake motions. Seismol. Bull. Central Meteorological Observatory Japan, 1, 92-122.

Okal, E. and Talandier, J.,1989. A variable-period mantle magnitude. Journal of Geophysical Research 94(B4): doi: 10.1029/88JB04010. issn: 0148-0227.

Okal, E. A., L. Dengler, S. Araya, J. C. Borrero, B. M. Gomer, S. Koshimura, G. Laos, D. Olcese, M. Ortiz , M. Swensson, V. V. Titov and F. Vegas, 2002. Field Survey of the Camaná, Perú Tsunami of 23 June 2001, Seismological Research Letters, November/December 2002, v. 73, p. 907-920

Ocola, L., 1966. "Earthquake Activity of Peru", Am. Geophys. U., Geophys. Monograph 10, 509-528.

Pararas-Carayannis, G, and A. S. Furumoto (1965). "Source Mechanism Study of the Alaska Earthquake and Tsunami of 27 March 1964, Part I, Water Waves", by G. Pararas-Carayannis; Part II. "Analysis of Raleigh Wave", by A. Furumoto, Rept. HIG65-17, 42 pp. Honolulu: Hawaii Inst. Geophys., Dec. 1965.

Pararas-Carayannis, G. (1968). "The Tsunami of October 17, 1966 in Peru", International Tsunami Information Center Newsletter, Vol. 1, No. 1, March 5.

Pararas-Carayannis, George 1969. Catalog of Tsunami in the Hawaiian Islands. World Data Center A-Tsunami

U.S. Dept. of Commerce Environmental Science Service Administration Coast and Geodetic Survey, May 1969.

Pararas-Carayannis, G., 1972. "The Great Alaska Earthquake of 1964 Source Mechanism of the Water Waves Produced", National Academy of Sciences - Committee on the Alaska Earthquake, Volume on Seismology and Geodesy, pp. 249-258.

Pararas-Carayannis, G., 1974. "An Investigation of Tsunami Source Mechanism off the Coast of Central Peru". Marine Geology, Vol. 17, pp. 235-247, Amsterdam: Elsevier Scientific Publishing Company. See also: http://drgeorgepc.com/Tsunami1966Peru.html

Pararas-Carayannis, George and Calebaugh P.J., 1977. Catalog of Tsunamis in Hawaii, Revised and Updated. World Data Center A – Tsunami report.

Pararas-Carayannis, G., 1996. The Earthquake and Tsunami of February 21, 1996 in Northern Peru. http://drgeorgepc.com/Tsunami1996Peru.html

Pararas-Carayannis, G., 2007. Earthquake and Tsunami of 15 August 2007 in Peru. http://www.drgeorgepc.com/Earthquake2007Peru.html

Pararas-Carayannis, G., 2010. Earthquake and Tsunami of 27 February 2010 in Chile - Evaluation of Source Mechanism and of Near and Far-field Tsunami Effects. Science of Tsunami Hazards", Vol. 29, No. 2, (2010)
http://www.drgeorgepc.com/Tsunami2010Chile.html

H. Perfettini, H., Avouac, J.P., and J.-C. Ruegg, 2005. Geodetic displacements and aftershocks following the 2001 *Mw* = 8.4 Peru earthquake: Implications for the mechanics of the earthquake cycle along subduction zones. JOURNAL OF GEOPHYSICAL RESEARCH, VOL. 110, B09404, 19 PP., 2005 doi:10.1029/2004JB003522.

Robinson, D.P., S. Das, S., and A. B. Watts, 2006. Earthquake Rupture Stalled by a Subducting Fracture Zone, Science 26 May 2006: Vol. 312 no. 5777 pp. 1203-1205

Rosenbauma G., Giles D., Saxon M., Betts P. G., Weinberg R. F., and C. Duboz, 2005A. Subduction of the Nazca Ridge and the Inca Plateau: Insights into the formation of ore deposits in Peru. Earth and Planetary Science Letters, Volume 239, Issues 1-2, 30 October 2005, Pages 18-3

Rosenbaum, G., Giles, D., Betts, P., Saxon, M., Weinberg, R., and C Duboz, 2005 B. American Geophysical Union, Fall Meeting 2005, abstract #T33B-0554,

Sacks I.S., 1983. The subduction of young lithosphere, J. Geophys. Res. 88 (1983) 3355-3366.

Sladen, A.; Madariaga, R.; Clévédé, E., 2004. Nonlinear Source Tomography Of The Mw=8.4, 23 June 2001 Arequipa, Peru Earthquake. *American Geophysical Union,Fall Meeting 2004, abstract #S53A-0181*